AGU PUBLICATIONS

JGR

Journal of Geophysical Research: Earth Surface

RESEARCH ARTICLE

10.1002/2016JF004087

Key Points:
- The Lagrangian and Eulerian approaches to bed load transport are merged into a unifying framework
- Conceptual derivations involve first moments of key quantities
- Lagrangian quantities that are difficult to measure can be deduced from Eulerian ones

Correspondence to:
F. Ballio,
francesco.ballio@polimi.it

Citation:
Ballio, F., Pokrajac, D., Radice, A., & Hosseini Sadabadi, S. A. (2018). Lagrangian and Eulerian description of bed load transport. *Journal of Geophysical Research: Earth Surface*, *123*, 384–408. https://doi.org/10.1002/2016JF004087

Received 20 SEP 2016
Accepted 3 FEB 2018
Accepted article online 13 FEB 2018
Published online 26 FEB 2018

Lagrangian and Eulerian Description of Bed Load Transport

Francesco Ballio[1], Dubravka Pokrajac[2], Alessio Radice[1], and Seyed Abbas Hosseini Sadabadi[1]

[1]Department of Civil and Environmental Engineering, Politecnico di Milano, Milan, Italy, [2]School of Engineering, University of Aberdeen, Aberdeen, UK

Abstract Sediment particles transported as bed load undergo alternating periods of motion and rest, particularly at weak flow intensity. Bed load transport can be investigated by either following the motion of individual particles (Lagrangian approach) or observing the phenomenon at prescribed locations (Eulerian approach). In this paper, the Lagrangian and Eulerian descriptions are merged into a unifying framework that includes definitions for quantities used to describe the kinematics of particle motion, as well as the relationships among these quantities. The alternation of motion and rest is represented by two complementary descriptions: (i) *proportion of motion,* indicating either the relative time spent in motion by an individual particle or the relative number of moving particles; (ii) *persistence of motion*, indicating the extent to which the process consists of relatively few long periods of motion or of many short ones. The framework only involves first moments of the key quantities. The conceptual developments are tested against results from an experiment with weak bed load transport, demonstrating the soundness of the approach. From an operational point of view, a Lagrangian observation is difficult to perform, since the particle motion is usually investigated for finite spatial domains (e.g., a measurement window within a laboratory or natural reach). Strategies to overcome such limitations are described, suggesting the possibility of obtaining unbiased mean values for Lagrangian descriptors. The proposed framework can be used in any study aimed at parameterizing the kinematic properties of bed load particles as functions of the hydrodynamic conditions.

1. Introduction

Lagrangian and/or Eulerian approaches can be used for the observation of motion. The former approach follows objects as they move, while the latter explores the process dynamics at prescribed locations. In the context of bed load sediment transport the two approaches correspond to following the trajectories of solid particles (e.g., Ancey et al., 2002; Campagnol et al., 2013; Fathel et al., 2015; Heays et al., 2014; Lajeunesse et al., 2010) and to characterizing the sediment transport properties at some place (e.g., Böhm et al., 2004; Garcia et al., 2007; Nelson et al., 1995; Radice et al., 2010, 2013), respectively. Typically, the Lagrangian approach is mostly used when dispersion of tracer particles comes into play (e.g., Campagnol et al., 2015; Fan et al., 2016; Fathel et al., 2016; Hassan et al., 2013; Lisle et al., 1998; Martin et al., 2012; Nikora et al., 2001, 2002), whereas the Eulerian approach is employed for the investigation of sediment fluxes (e.g., Ancey & Heyman, 2014; Ballio et al., 2014; Cohen et al., 2010; Frey et al., 2003; Furbish, Haff, et al., 2012; Radice, 2009; Singh et al., 2009; Turowski, 2010).

The two approaches complement each other because they provide alternative descriptions of the process. For example, let one consider the sediment transport rate: it has been expressed in a fully Eulerian form as proportional to a bed load sediment concentration and a sediment velocity, or in a Lagrangian-Eulerian form as proportional to an Eulerian entrainment rate and a Lagrangian hop length (e.g., Garcia, 2008). Conditions of equivalence for the two expressions have been discussed in the literature from a variety of perspectives and under different restricting conditions (e.g., Ancey et al., 2006; Blom & Parker, 2004; Furbish, Roseberry, et al., 2012).

More generally, the identification of conceptual links between the Lagrangian and Eulerian approaches to bed load transport has been important for analyzing the complexity of processes in sediment mechanics since the pioneering work of Einstein (1937). Recent studies on this topic (e.g., Ancey & Heyman, 2014; Ancey et al., 2008; Furbish, Roseberry, et al., 2012; Ganti et al., 2009; Niño & Garcia, 1998; Voepel et al., 2013) have made extensive use of mathematical and/or statistical approaches to describe the richness of the sediment transport process.

From an operational point of view, measurements of Lagrangian and Eulerian indicators of particle motion pose several key issues. In both approaches, the mass of the particle can be concentrated into an infinitesimal volume or distributed within a finite volume (e.g., Ancey et al., 2008; Ballio et al., 2014; Berzi et al., 2015; Campagnol et al., 2012; Charru et al., 2004; Fan et al., 2014; Kempe & Fröhlich, 2012; Wu & Chou, 2003). Furthermore, Eulerian variables are typically (though not necessarily) defined over a control volume and a time scale: for example, an entrainment rate can be operationally determined by assessing if one or more particles have been entrained from a certain area within a certain time interval (e.g., Cao, 1997; Hosseini Sadabadi et al., 2016a; Van Rijn, 1984). The requirement of a control volume and time scale for the measurement entails determining the scaling properties of the various quantities (e.g., Bunte & Abt, 2005; Campagnol et al., 2012; Radice et al., 2009; Singh et al., 2009). Moreover, measurements are always performed within finite domains (in both space and time). These domains are larger than the measurement scales presented above (e.g., experiment duration is larger than a time interval used for measurement; analogously, the length of an investigated reach is larger than control volumes used to measure any quantity within the same reach). Experimental results can, however, depend on the extent of these finite domains. In this regard, the most appropriate experimental conditions to correctly identify Lagrangian properties (that should not depend on spatial and temporal constraints) are far from ascertained (e.g., Fathel et al., 2015). In principle, linking the Eulerian and Lagrangian approaches can help overcome operational limitations for measurement of Lagrangian quantities.

The aim of this paper is to explore the links between Lagrangian and Eulerian kinematic variables. The problem is well resolved in the classic continuum framework, where (Lagrangian) velocities of infinitesimal units of mass are linked to the (Eulerian) velocity field. In sediment transport problems, the classic approach may fail for weak transport conditions or when relatively high time and space resolutions are required. In such cases, the process may not be treatable as a mathematical continuum because variables become highly irregular (e.g., Ancey, 2010; Ballio et al., 2014; Böhm et al., 2004; Coleman & Nikora, 2009; Fathel et al., 2015; Lisle et al., 1998). More specifically, conceptualizations of sediment mechanics at the particle scale require taking into account process intermittency, which we identify with the alternation of motion and rest periods resulting from entrainment and disentrainment events (in other words, the term "intermittent" is used here for quantities with values that alternate between zero, during some time intervals, and nonzero, during others).

Studies of sediment mechanics do not rely solely on the time series of (Lagrangian or Eulerian) sediment velocities. A variety of derived variables are also used to describe the complexity of sediment kinematics (examples of these variables are hop lengths and time intervals, concentrations of moving particles, time- and space-averaged grain velocities, sediment pickup and deposition rates, and solid fluxes). Such derived variables represent fundamental information about sediment kinematics (how many particles are in motion and how quickly they move) that, while expressed in different ways, may be correlated with one another.

The research question of this paper, therefore, can be formulated as follows: how can one derive a set of quantities, involved in Lagrangian or Eulerian models for sediment transport, from the kinematics of individual grains and provide a unifying framework linking the two (Lagrangian and Eulerian) approaches? This sort of framework is important for two reasons. First, the framework supports interpretation and comparison of different expressions for sediment kinematics due to the choice of different combinations of variables. Second, the framework supports experimental investigation of sediment transport processes because variables that cannot be directly measured may be estimated indirectly through their links with other variables.

To answer the above research question, we propose a consistent kinematic framework where: (i) restrictive hypotheses are kept to a minimum; (ii) links are defined for deterministic variables (instantaneous and/or time averaged); (iii) only first moments of the quantities are considered; and (iv) all the parameters commonly used in sediment transport studies are considered, as well as their mutual relationships.

To the best of our knowledge, the existing literature proposes relatively few solutions to this problem, and none of them has the characteristics of the one presented here. Recent approaches (e.g., Ancey & Heyman, 2014; Ancey et al., 2006; Fan et al., 2014; Furbish, Roseberry, & Schmeeckle, 2012; Lajeunesse et al., 2010) are devoted to the definition of the stochastic properties of some variables and, with respect to the present work, account for more statistical moments of fewer quantities.

The paper is organized as follows: section 2 specifies the general framework of the approach by defining the fundamental variables and operators. Sections 3 and 4 present derivations of averaged quantities. In particular, various tools are employed in order to account for the intermittency of the sediment transport process, which is here a synonym for the alternation between states of particle motion and rest. An application of the framework to analyzing experimental data is conducted in section 5, where a method is also described to appropriately compute Lagrangian quantities (Lagrangian proportion of motion and hop properties) from an observation over a finite domain. A discussion of critical issues and the major conclusions are provided in the subsequent sections.

2. Conceptual Framework

We consider identical grains transported as one-dimensional bed load. These grains represent an arbitrary sample from the population of all the sediment involved in the process as, for example, a given grain size class, or a tracer. For simplicity, grains are assumed to move only in the positive x direction.

The Lagrangian description of bed load is based on the kinematics of individual particles. Values of involved quantities, such as the number of particles or their velocity, are then integrated/averaged in space for the Eulerian description over a control volume. The higher the number of particles present in the control volume, the smoother the temporal variations of quantities obtained.

Definitions presented in this paper do not require an assumption of a large number of particles involved. They allow taking into account the rarefied transport conditions that often occur in both natural and experimental settings. However, a large number of particles in the control volume is typically necessary for the quantities obtained by integration/averaging over this volume to be physically meaningful.

As noted above, bed load sediment transport is an intermittent process. Therefore, two main states of motion and stillness must be appropriately accounted for. In this study, many kinematic descriptors will be defined considering only the moving particles. The following main concepts will be introduced:

1. *Proportion of motion* (section 3), indicating the relative occurrence of motion and stillness, thus furnishing "large-scale" information about particle activity. Proportion of motion can be defined for a single particle (time the particle spent in motion relative to the entire observation time) or for a set of particles (relative number of moving particles within a sample).
2. *Persistence of motion* (section 4), indicating if the process consists of many short events or a few longer ones. This concept can be applied to single or multiple particles.

Summarizing the above considerations, the manuscript will be articulated by using two conceptual axes, one related to the reference frame (Lagrangian or Eulerian) and one to the description of intermittency (by proportion or persistence of motion). Four combinations will thus be explored, as well as the relationships among them.

2.1. Lagrangian Description

An individual particle is denoted with i and the total number of particles in the sample is N. The streamwise position of a particle at any time t (Figure 1a) is denoted with $x(i,t)$. For the ith particle, one can identify a succession of alternating periods of movement and rest. A single period of motion and the following period of rest (Figure 1b) form an "event." $J(i)$ indicates the total number of events in the history of the particle. The duration of the jth event for the ith particle is $\Delta t(i,j)$, and it can be further split into durations of motion and stillness (rest), $\Delta t^m(i,j)$, and $\Delta t^r(i,j)$, respectively. Similarly, $\Delta x(i,j)$ represents the displacement of a particle i during an event j, which is often referred to as "hop length."

At any instant a particle i may or may not be in a state of motion. Therefore, it is convenient to introduce a "clipping function" M^m to quantify the state of motion of the ith particle as

$$M^m(i,t) = \begin{cases} 1 & \text{if particle is moving} \\ 0 & \text{if particle is not moving} \end{cases} \quad (1)$$

The clipping function M^m can be expressed as

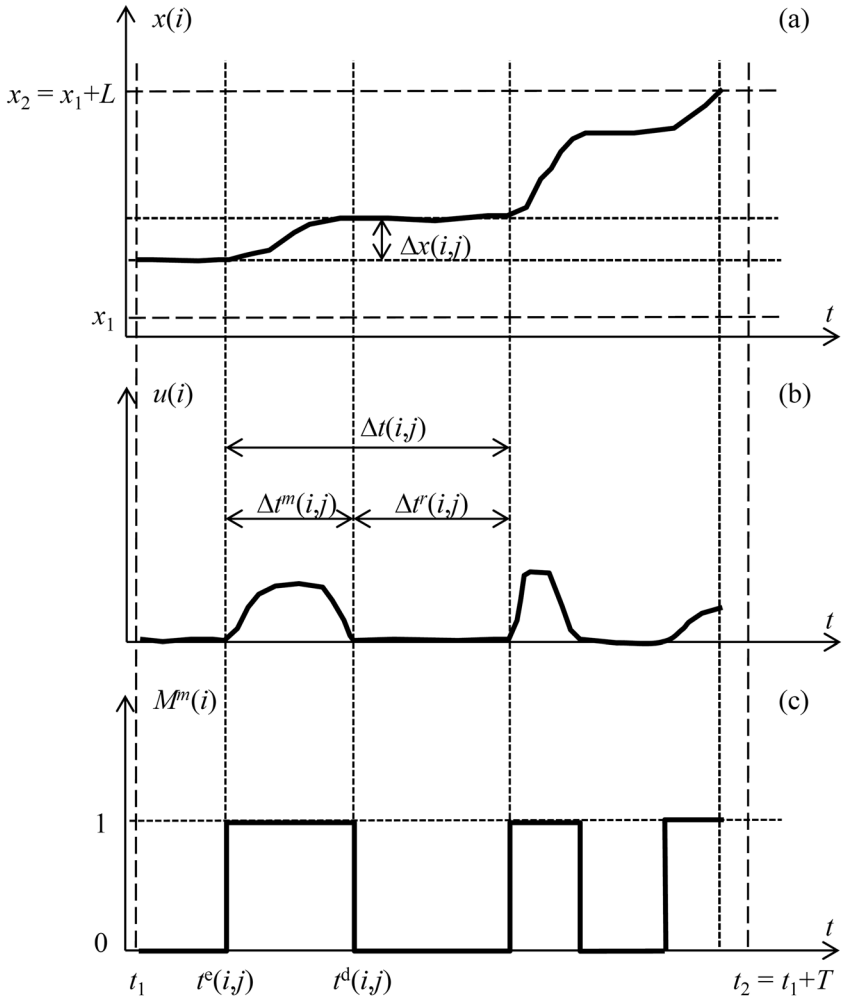

Figure 1. Conceptual description of an *i*th particle path by its (a) position *x*, (b) velocity *u*, and (c) clipping function for motion M^m. Properties of a *j*th event (time of motion and rest, total duration, displacement length, instants of entrainment and disentrainment) are sketched. The long dashed lines mark an Eulerian observation window.

$$M^m(i,t) = \sum_j \left[\mathrm{H}(t - t^{\mathrm{e}}(i,j)) - \mathrm{H}\left(t - t^{\mathrm{d}}(i,j)\right)\right], \tag{2}$$

where $t^{\mathrm{e}}(i,j)$ and $t^{\mathrm{d}}(i,j)$ identify the instants of entrainment (pickup) and disentrainment (deposition), respectively, for an event *j*, and H() is the Heaviside step function. An example of a temporal evolution of M^m is shown in Figure 1c. The time derivative of $M^m(i,t)$ is

$$\frac{\mathrm{d}M^m(i,t)}{\mathrm{d}t} = \sum_j \delta(t - t^{\mathrm{e}}(i,j)) - \sum_j \delta\left(t - t^{\mathrm{d}}(i,j)\right) = e(i,t) - d(i,t), \tag{3}$$

where δ is a Dirac delta function that can be used to define $e(i,t)$ and $d(i,t)$ (i.e., entrainment and disentrainment functions, respectively) for the particle.

The distinction between the states of stillness and motion identifies whether a grain belongs to the static bed or to the transport layer, thus defining two subsamples of particles. Due to this simplified description of the states of motion, transitions from the one state to the other one (entrainment and disentrainment) imply finite variations of extensive quantities (e.g., number of particles and corresponding total volume or mass) pertaining to each subsample within infinitesimal times. Time series of these extensive quantities are thus discontinuous.

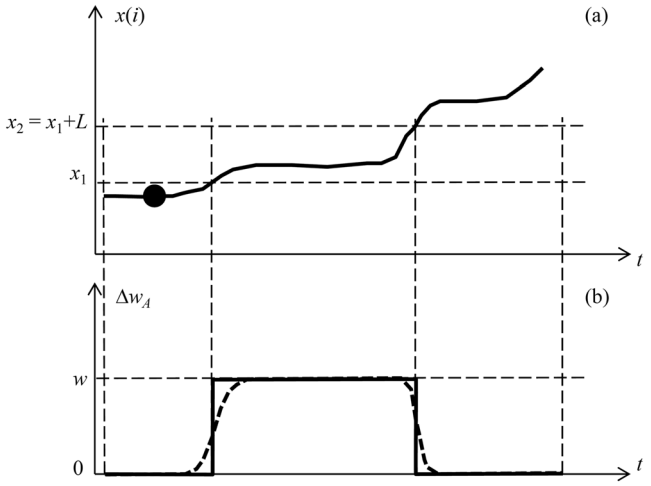

Figure 2. (a) Sketch of a particle moving through the reference plan area of the bed (bounded by x_1 and x_2); (b) the variation of the solid volume pertaining to the area, Δw_A, is depicted in two different scenarios of a distributed (finite) particle (thick dashed line) and a concentrated (infinitely small) particle (thick solid line).

2.2. Eulerian Description

A control volume for the Eulerian description may be chosen as a prism with vertical edges; relevant boundaries for sediment fluxes will be vertical surfaces. For simplicity, we now project the control volume onto a horizontal surface, thus transforming it into an area and its boundaries into lines. Bearing this in mind, consider a reference plan area A extending between two x-locations, x_1 and $x_2 = x_1 + L$ (Figure 2a) and having a certain width B. When a moving particle with volume w crosses the boundaries of A, the solid volume pertaining to A, w_A, changes (Figure 2b). This change can be described in two ways, depending on the conceptual model of the particle. If one considers a particle of a finite size (a distributed particle), the variation of the solid volume pertaining to A, Δw_A, grows continuously until it reaches w (i.e., until the whole particle has entered A; this is depicted by the thick dashed line in Figure 2b). Alternatively, all the properties of the particle (mass, volume, velocity, …) may be attributed to its center of mass (concentrated properties), so that the particle itself is considered infinitely small. The latter choice is simpler because it avoids having to account for the partial contribution of the particle's properties to the Eulerian values over A. For example, the whole volume of the particle, w, is added instantaneously to the solid volume pertaining to A, at the moment when the particle center crosses the upstream boundary of A. This in turn generates discontinuities in the time series whenever the center of mass crosses either boundary of A (solid lines in Figure 2b). In this paper, we adopt the latter approach, where all the properties of a particle are attributed to its center of mass.

To identify whether a particle i is within the reference area A, an Eulerian clipping function is defined as

$$M^A(i,t) = \begin{cases} 1 & \text{if particle is within } A \text{ at time } t \\ 0 & \text{if particle is not within } A \text{ at time } t \end{cases}. \tag{4}$$

The total number of particles within A at time t is expressed as

$$N_A(t) = \sum_{i=1}^{N} M^A(i,t), \tag{5}$$

and the number of particles within A that are in motion at time t as

$$N_A^m(t) = \sum_{i=1}^{N} M^A(i,t)\ \ M^m(i,t) = \sum_{i=1}^{N_A(t)} M^m(i,t). \tag{6}$$

In analogy with equation (6) we can also define the number of particles at rest within A at time t as

$$N_A^r(t) = \sum_{i=1}^{N} M^A(i,t)\ \ (1 - M^m(i,t)) = \sum_{i=1}^{N_A(t)} (1 - M^m(i,t)). \tag{7}$$

For the Eulerian description it is also useful to express the volumetric sediment flux through a target transverse line located at $x = x_0$. This can be done by following the motion of a single grain as it approaches the target (with $u_i > 0$). The time at which this grain arrives at the target line is denoted with $t_0(i)$. The volumetric sediment flux through the target surface is expressed by including the contribution of each grain. For any ith grain to contribute to the total volume that passes through the target during a short period dt, its arrival time $t_0(i)$ must be within this interval, (i.e., $t \le t_0(i) \le t + \mathrm{d}t$). The total volume of all the particles satisfying this condition is expressed as

$$\mathrm{d}V = w\left[\sum_{i=1}^{N} \mathrm{H}(t + \mathrm{d}t - t_0(i)) - \sum_{i=1}^{N} \mathrm{H}(t - t_0(i))\right] = w\sum_{i=1}^{N} \mathrm{dH}(t - t_0(i)) = w\sum_{i=1}^{N} \delta(t - t_0(i))\mathrm{d}t, \tag{8}$$

where w is again the particle volume. The first term within square brackets is the number of particles beyond the line at $t + \mathrm{d}t$, while the second is the number of particles already beyond the line at t. The instantaneous discharge, therefore, is equal to

$$Q = \frac{\mathrm{d}V}{\mathrm{d}t} = w \sum_{i=1}^{N} \delta(t - t_0(i)) = w \sum_{i=1}^{N} u(i,t)\delta(x(i,t) - x_0) \tag{9}$$

The instantaneous sediment discharge is represented by delta functions and, therefore, is discontinuous in time, like the entrainment and disentrainment functions defined by equation (3). In this case, the discontinuity is due to considering concentrated particles, while considering particles with a finite volume would have led to a continuous time series of Q as was comparatively shown, for example, by Campagnol et al. (2012).

2.3. Averaging Options

Considering the sparseness in space and intermittency in time of sediment motion, first moments of Lagrangian and Eulerian descriptors of sediment motion can be obtained through various forms of averaging. The following averaging options are considered here, in which θ indicates any general quantity.

Time averaging provides integrated properties, smoothing temporal fluctuations:

$$\overline{\theta} = \frac{1}{T} \int_{t}^{t+T} \theta(t)\,\mathrm{d}t. \tag{10}$$

It should be noted that the quantity θ in equation (10) may be a property of a single grain or of a set of grains.

Sample averaging yields quantities that are averaged over a set of individual particles:

$$\{\theta\} = \frac{1}{N} \sum_{i=1}^{N} \theta(i), \tag{11}$$

$$\{\theta\}_A = \frac{1}{N_A} \sum_{i=1}^{N_A} \theta(i). \tag{12}$$

One should consider that sample averaging by equation (11) is a fully Lagrangian operator, while averaging by equation (12) includes a dependency on A and is thus a mixed Lagrangian/Eulerian operator.

Finally, expected values will be associated with averaging in the space of realizations (e.g., experiment repetitions) and will be denoted with square brackets, $[\theta]$.

The above definitions consider any quantity as a function of time t, a particle i, and a realization. A further averaging option is here defined, since at any time t a particle experiences its jth motion event (see again Figure 1). *Event averaging* provides an alternative to equation (10), yielding properties of particle hops (or of rest terms as their counterparts):

$$\langle\theta\rangle = \frac{1}{J} \sum_{j=1}^{J} \theta(j), \tag{13}$$

recalling that J is the number of observed events for the particle. The averaging option (13) is limited to Lagrangian quantities, as it considers a succession of particle motion events.

In ideal (uniform, stationary, and ergodic) conditions, and when the spatial and temporal windows and the size of ensembles are sufficiently large, corresponding averaging options produce identical statistics (e.g., Von Plato, 1991). However, experimental conditions always impose operational limitations (small averaging area, short observation time) and, therefore, can result in biased average values. In such conditions, temporal and sample averaging may be used to complement each other (e.g., by applying them successively) and, hence, produce estimates of mean values better than either of them would produce on its own. In what follows, temporal and sample averaging will be considered together, jointly representing the general population.

3. Proportion of Motion

This section explores global quantities that describe the relative importance of the states of motion and rest. By way of introduction, Figure 3 shows a conceptual description of motion for a set of N concentrated

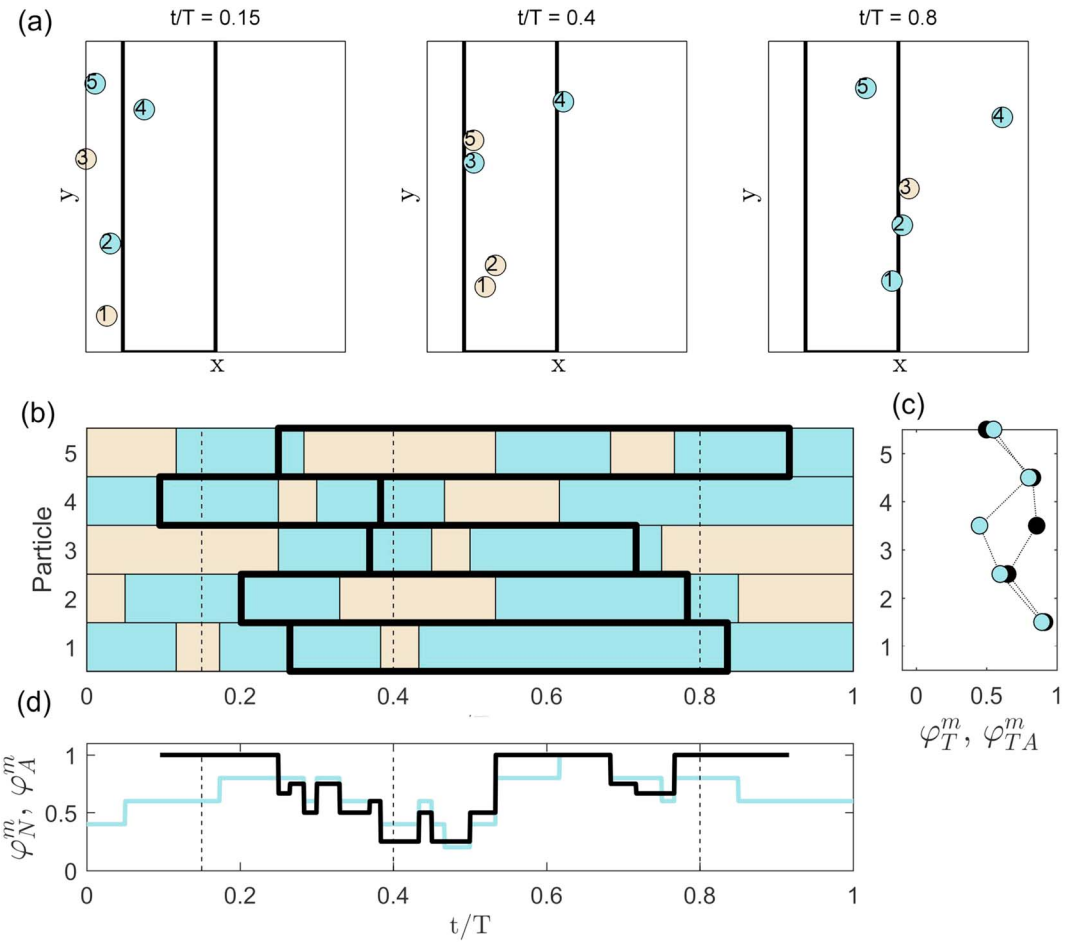

Figure 3. Conceptual description of motion for a sample of N particles ($1 \le i \le N$) observed during the period $t_1 = 0 \le t \le t_2 = t_1 + T$, and above a plan area, A. (a) The particles at three time instances marked with dashed vertical lines in (b) and (d). The moving particles are colored blue and those at rest are beige. The boundaries of the area A are shown as thick black lines; (b) state of motion for all particles i throughout the observation period T: blue sections indicate motion and beige means rest; the thick black line encloses the period that the particle spent within the area A; (c) relative duration (with respect to T) of the state of motion, for each particle, $\varphi_T{}^m(i)$ (blue symbols), and for particles within A, $\varphi_{TA}{}^m(i)$ (black symbols); (d) relative number of particles in motion within the whole sample N, $\varphi_N{}^m(t)$ (blue line), and within the area A, $\varphi_A{}^m(t)$ (black line), versus time.

particles observed during a period T, and within a reference plan area A. Motion is indicated with blue color, while the beige color indicates rest. Figure 3a shows the particle locations at three time instants, as well as the boundaries of the area A. Figure 3b shows the state of motion for all particles throughout T, and a thick black line encloses the period that the particle spent within A. These diagrams are used as visual aids for definition of various Lagrangian and Eulerian quantities presented in sections 3.1 and 3.2, respectively, and sketched in Figures 3c and 3d. These are further developed in section 3.3, which analyzes the average sediment discharge.

3.1. Lagrangian Description of Movement for a Group of Particles

A Lagrangian perspective means that an observer follows a particle i or a group of particles (with $i = 1, 2, \ldots, N$) as they move (for example, the group of $N = 5$ particles shown in Figure 3a). We are interested in comparing the total duration of motion and rest periods of such a group of particles during an observation period of duration T ($t_1 < t \le t_1 + T$). The time that a particle i spends in motion during this period is equal to

$$T^m(i) = \int_{t_1}^{t_1+T} M^m(i,t)\,\mathrm{d}t. \tag{14}$$

The motion time $T^m(i)$ can be visualized in Figure 3b as the total length of the blue sections in the row plotted against particle *i*. The corresponding relative time spent in motion, $\varphi_T{}^m(i)$, (equal to the time spent in motion divided by the total observation time) can be defined as

$$\varphi_T^m(i) = \frac{T^m(i)}{T} = \overline{M^m(i,t)}. \tag{15}$$

This relative time of motion was mentioned, for example, in Papanicolaou et al. (2002) and Ancey et al. (2006). A sketch of $\varphi_T{}^m$ for all particles is shown in Figure 3c with blue symbols. An analogous quantity $\varphi_{TA}{}^m(i)$, shown with black symbols in the same diagram, indicates the relative time that particle *i* spends in motion while it is within the reference area *A*; this mixed Lagrangian-Eulerian quantity will be defined in section 5.

On the other hand, for a group of *N* particles we can also define an instantaneous relative number of particles in motion, $\varphi_N{}^m(t)$ (equal to the number of moving particles divided by the total number of observed particles) as

$$\varphi_N^m(t) = \frac{N^m(t)}{N} = \frac{\sum_{i=1}^{N} M^m(i,t)}{N} = \{M^m(i,t)\}, \tag{16}$$

where N^m is the number of particles in motion. In Figure 3a, the number of moving particles at three different instants is 3, 2, and 4, out of 5, hence yielding $\varphi_N{}^m = 0.6$, 0.4, and 0.8, respectively. A sketch of $\varphi_N{}^m$ during the entire period of observation is shown in Figure 3d as a blue line. Since only five particles are observed, the $\varphi_N^m(t)$ diagram shows a step change of 0.2 every time a particle starts or stops moving.

If the process is ergodic, stationary, and uniform in space, it is physically meaningful to look for the expected value of the proportion of motion, ϑ^m, defined as

$$\vartheta^m = [M^m(i,t)]. \tag{17}$$

This quantity indicates how likely a particle *i* is to be moving at a time instant *t* (i.e., in how many realizations, relative to a large total number of realizations, the particle has been moving at time *t*). For a stationary and spatially uniform process, the value of ϑ^m is the same for all particles and all time instances, so that one can also call it a global proportion of motion and estimate its value by equation (15) or (16).

In order to obtain a good estimate of the global relative duration of motion, ϑ^m, we need a sufficiently large data set in terms of the number of particles and the length of observation time compared to typical periods of motion and rest. In the absence of large samples, it can be easily shown that the sample average of $\varphi_T{}^m$ is equal to the time average of $\varphi_N{}^m(t)$:

$$\{\varphi_T^m\} = \overline{\varphi_N^m} = \frac{1}{N}\frac{1}{T}\sum_{i=1}^{N}\int_{t_1}^{t_1+T} M^m(i,t), \tag{18}$$

and this nested sample and time averaging can be employed to obtain an estimate of ϑ^m as

$$\vartheta^m \cong \left\{\overline{M^m(i,t)}\right\} = \{\varphi_T^m\} = \overline{\varphi_N^m}. \tag{19}$$

3.2. Eulerian Description of Movement Within a Reference Spatial Domain

From an Eulerian perspective we are interested in describing the state of motion within the reference area *A*. We, therefore, define the relative number of particles within the reference area *A* that are moving, $\varphi_A{}^m(t)$ (equal to the number of moving particles within *A* divided by the total number of particles within *A*):

$$\varphi_A^m(t) = \frac{N_A^m(t)}{N_A(t)} \tag{20}$$

For example, the middle diagram in Figure 3a shows four particles within the area *A*, and only one of them is moving, so that the corresponding $\varphi_A{}^m$ value is 0.25. A sketch of $\varphi_A{}^m$ during the entire period of observation is shown in Figure 3d as a black line. It shows a step change every time a particle changes the state of motion, or enters into *A*, or exits from it.

A particle i is within A when the clipping function $M^A(i,t)$ is equal to 1 (within black boxes in Figure 3b), and it is moving when $M^m(i,t) = 1$. Therefore, the relative number of moving particles within A, ${\varphi_A}^m$, also can be expressed as

$$\varphi_A^m(t) = \frac{\sum_{i=1}^{N_A(t)} M^m(i,t)}{\sum_{i=1}^{N} M^A(i,t)} = \frac{\sum_{i=1}^{N} M^A(i,t)\, M^m(i,t)}{\sum_{i=1}^{N} M^A(i,t)} = \frac{\{M^A(i,t)\ \ M^m(i,t)\}}{\{M^A(i,t)\}} \tag{21}$$

The Lagrangian quantities ${\varphi_T}^m$ and ${\varphi_N}^m$, and the Eulerian quantity ${\varphi_A}^m$, quantify the proportion of motion in different manners. For an integrated approach, it is interesting to explore the conditions under which ${\varphi_T}^m$, ${\varphi_N}^m$, and ${\varphi_A}^m$ become estimates of ϑ^m. One possibility is to use a time average of ${\varphi_A}^m(t)$, which is analogous to using the Lagrangian quantity $\overline{\varphi_N^m}$ equation (18), except that now the state of motion is observed above an area A. For the ideal case of A being "large," $N_A(t)$ is also large, and we can assume that it is constant in time (e.g., Ancey et al., 2006; Furbish, Roseberry, et al., 2012): $N_A(t) \cong N_A$. It follows from equation (20) or (21) that

$$\varphi_A^m(t) = \{M^m(i,t)\}_A \tag{22}$$

and φ_A^m also tends to be constant in time. Moreover, if N_A is large, we can assume that $\{M^m(i,t)\} = \{M^m(i,t)\}_A$ (i.e., averaging over the set of particles within A produces the same result as averaging over the entire sample N). This means that $\varphi_A^m(t) = \varphi_N^m(t)$. Hence, the relationship with the Lagrangian relative time of motion for a particle and the global expected relative duration of motion expressed by equation (19) applies.

In the case of a "small" area, instead, a further issue arises because the total number of particles used to obtain ${\varphi_A}^m(t)$, $N_A(t)$, may vary with time. The time-varying number of particles, $N_A(t)$, can be decomposed into a time average:

$$\overline{N_A(t)} = N\,\overline{\{M^A(i,t)\}}, \tag{23}$$

and a fluctuation, $N_A'(t) = N_A(t) - \overline{N_A(t)}$. This, in turn, produces correlation terms in the expression for the time average of the number of moving particles within A, $N_A^m(t)$, which can be developed as

$$\overline{N_A^m(t)} = \overline{\sum_{i=1}^{N_A(t)} M^m(i,t)} = \overline{N_A(t)\{M^m(i,t)\}_A} = \overline{N_A(t)}\ \overline{\{M^m(i,t)\}_A} + \overline{N_A'\{M^m\}_A'}, \tag{24}$$

The expression for $\overline{\varphi_A^m(t)}$ can be found by averaging equation (20) in time and combining it with equations (23) and (24).

3.3. Sediment Discharge and Effective Velocities

This section presents the relationship between the sediment motion and the sediment discharge through a target line located at x_0. The time average sediment discharge through the target line during the period of observation $t_1 \le t \le t_2 = t_1 + T$ can be expressed as

$$\overline{Q}(t_1,t_2) = \frac{V(t_1,t_2)}{t_2 - t_1} = \frac{w}{T} N_Q \tag{25}$$

where N_Q is the number of particles crossing the target line during the observation period T. The derivation of the expected value of N_Q and $\overline{Q}$ is presented in Appendix A. It has been carried out under the assumption that the area A used to calculate N_A/A is sufficiently large to provide stable values and also that N_A/A is constant in space. From equation (A4) the expected value of sediment discharge per unit width is

$$\frac{[\overline{Q}]}{B} = w \frac{N_A}{A} \frac{[\lambda]}{T}, \tag{26}$$

where B is a reference width and λ is the distance traveled by one particle during T. If we denote wN_A/A with C, the expected value of the sediment transport rate can be expressed as

$$\frac{[\overline{Q}]}{B} = C[u], \tag{27}$$

where u is a (Lagrangian) effective velocity of particles equal to λ/T. The ratio of the distance to the part of T during which the particle was moving, T^m, yields the time-averaged velocity of particles during motion, u^m, which is related to the effective velocity by

$$\overline{u^m} = \frac{\overline{u}}{\varphi_T^m}. \tag{28}$$

When the area A is not sufficiently large to consider N_A as constant, a correlation term must be added to equation (27). As discussed in Ballio et al. (2014), if one considers an instantaneous solid discharge equal to the product of instantaneous concentration and velocity ($Q/B = Cu$), then the time-averaged solid discharge is

$$\frac{\overline{Q}}{B} = \overline{C}\,\overline{u} + \overline{C'u'}, \tag{29}$$

where the correlation term can be interpreted as a diffusive flux (e.g., Ancey & Heyman, 2014; Furbish, Roseberry, et al., 2012; Heyman et al., 2016). The relative weight of the mean and fluctuating terms in equation (29) may also depend on the choice of the variables. For example, Radice and Ballio (2008) presented an analysis of experimental data and a corresponding formalism according to which the use of u^m rather that u made the correlation vanish. This finding was interpreted by arguing that concentration and velocity are highly correlated in relation to the intermittency of the process (they are either both equal to zero or different from zero at any instant in time), but may not be correlated when only the period in motion is considered (i.e., when they are both different from zero).

4. Persistence of Motion

As a counterpart of section 3, which presented a global proportion of motion, the present section provides a more detailed description. We want to distinguish a highly variable behavior (consisting of many occurrences of relatively short periods of motion and rest) from another behavior with a less frequent exchange of longer periods of motion and rest. In the latter case, a particle, once entrained, tends to remain in motion for a longer period of time (i.e., to persist in motion). This tendency is, therefore, referred to as persistence of motion. The approach taken in this section is an alternative way to account for the intermittence of the bed load process. It is closely related to an entrainment-disentrainment form of the Exner equation (e.g., Ancey, 2010; Ancey & Heyman, 2014; Ballio et al., 2014; Charru et al., 2004; Lajeunesse et al., 2010), as well as to modeling the particle trajectories as random walks (e.g., Fan et al., 2016; Lisle et al., 1998). From a phenomenological point of view, the persistence of motion is also obviously related to the characteristics of particle hops (e.g., Campagnol et al., 2015; Fathel et al., 2015; Hu & Hui, 1996; Lee et al., 2000; Ramesh et al., 2011).

4.1. Lagrangian Variables

Particle behavior is here analyzed at the scale of the "intermediate trajectories" according to the conceptual definition by Nikora et al. (2001, 2002). These correspond to the hop lengths and the associated individual periods of motion interrupted by periods of rest. The time window of observation T is, necessarily, much larger than the time scales of both periods.

With reference to Figures 1a and 1b, a hop length of a particle i corresponds to an event that consists of a single period of motion followed by a single period of rest, so that the duration of such an event is $\Delta t = \Delta t^m + \Delta t^r$. Note that, by definition, an event contains a single entrainment (of a particle being at rest) and a single disentrainment (of the same particle, moving after entrainment). The average effective velocity of the particle during the event is $u_{\Delta x} = \Delta x/\Delta t$, while its counterpart during the period of motion is ${u_{\Delta x}}^m = \Delta x/\Delta t^m$.

The total time of movement for a particle i during period T, $T^m(i)$, has been defined by equation (14). Alternatively, hop-related quantities can be used to express $T^m(i)$ as

$$T^m(i) = \sum_{j=1}^{J(i)} \Delta t^m(i,j). \tag{30}$$

The total time of rest for the particle i during T is analogous:

$$T^r(i) = \sum_{j=1}^{J(i)} \Delta t^r(i,j). \tag{31}$$

Assuming that T is large enough to disregard truncated periods of motion/rest at the beginning and at the end of the time window, it follows that for each particle i

$$T(i) = T^m(i) + T^r(i) = \sum_{j=1}^{J} \Delta t(i,j) = J(i)\langle \Delta t(i,j)\rangle. \tag{32}$$

The relative duration of motion along the global trajectory, which is expressed by equation (15) as $\varphi_T{}^m = T^m/T$, does not provide information about how persistent the motion is (i.e., to what extent it is partitioned into short or long intervals). Instead, the persistence of motion can be quantified by the time averaging of Lagrangian entrainment or disentrainment functions:

$$\overline{e}(i) = \frac{1}{T}\int_{t_1}^{t_1+T} e(i,j)\mathrm{d}t = \overline{d}(i) = \frac{1}{T}\int_{t_1}^{t_1+T} d(i,j)\mathrm{d}t = \frac{J(i)}{T} = \frac{1}{\langle \Delta t(i,j)\rangle}. \tag{33}$$

In other words, if the intermediate trajectories for a given particle have an average duration $\langle \Delta t\rangle$, the average rate of events (entrainment, disentrainment) is $1/\langle \Delta t\rangle$. Equation (33) is an example of connecting time averaging with event averaging, consistent with arguments in section 2.3. One should note that time averages for $e(i,t)$ and $d(i,t)$ along the trajectory have to be equal, because each event contains a single entrainment and a single disentrainment and, therefore, the total number of entrainments during the period T is the same as the number of disentrainments, and at the same time the same as the number of events, $J(i)$.

As described above, there are various options for averaging. For uniform conditions in space and time, and in the presence of a sufficiently large sample characterized by ergodic processes, all averages converge to expected values:

$$\langle \Delta t^m\rangle = \{\Delta t^m\} = [\Delta t^m] = \tau^m, \tag{34a}$$

$$\langle \Delta t^r\rangle = \{\Delta t^r\} = [\Delta t^r] = \tau^r, \tag{34b}$$

$$\langle \Delta t\rangle = \{\Delta t\} = [\Delta t] = \tau = \tau^m + \tau^r. \tag{34c}$$

This also applies to multiple subsequent averages, as, for example, in equation (19). A consequence of equations (34a)–(34c) is that the expected value of the proportion of motion also can be expressed as $\vartheta^m = \tau^m/\tau$.

For hop length, one obtains:

$$\lambda(i) = \sum_{j=1}^{J(i)} \Delta x(i,j), \tag{35}$$

so that $\lambda(i) = J(i)\langle \Delta x(i,j)\rangle$. We can define different averages for Δx, all converging to an expected value:

$$\langle \Delta x(i,j)\rangle = \{\Delta x(i,j)\} = [\Delta x(i,j)] = \xi. \tag{36}$$

Some attention to particle velocities is required because the average velocity of a particle when it is in motion, u^m, is different from the event-averaged velocity along intermediate trajectories:

$$\overline{u^m(i)} = \frac{\lambda(i)}{T^m} = \frac{\sum_{j=1}^{J(i)} \Delta x(i,j)}{\sum_{j=1}^{J(i)} \Delta t^m(i,j)} = \frac{\langle \Delta x(i,j)\rangle}{\langle \Delta t^m(i,j)\rangle} \neq \left\langle \frac{\Delta x(i,j)}{\Delta t^m(i,j)} \right\rangle = \left\langle u^m_{\Delta x}(i,j)\right\rangle. \tag{37}$$

The inequality is due to the fact that the intermediate trajectories (hops), $\Delta x(i,j)$, are typically correlated with the corresponding time of motion, $\Delta t^m(i,j)$ (e.g., Fathel et al., 2015).

4.2. Eulerian Variables: Entrainment/Disentrainment

A derivation of Eulerian entrainment and disentrainment functions, *E(t)* and *D(t)*, from their Lagrangian counterparts is analogous to the derivation presented for the number of particles in motion over *A* (see again equation (21)):

$$E(t) = \sum_{i=1}^{N} M^A(i,t)e(i,t) = \sum_{i=1}^{N_A(t)} e(i,t) = \sum_{i=1}^{N_A^r(t)} e(i,t), \tag{38}$$

$$D(t) = \sum_{i=1}^{N} M^A(i,t)d(i,t) = \sum_{i=1}^{N_A(t)} d(i,t) = \sum_{i=1}^{N_A^m(t)} d(i,t). \tag{39}$$

Note that summing $e(i,t)$ over either N_A or ${N_A}^r$ gives the same result, since an already moving particle cannot be entrained. Analogously, summing $d(i,t)$ over either N_A or ${N_A}^m$ also yields the same result.

Temporal evolutions for *E* and *D* are discontinuous, analogous to those for *e* and *d* described above. If previous definitions are averaged in time, one obtains:

$$\overline{E} = \sum_{i=1}^{N} \overline{M^A(i,t)e(i,t)} = \overline{\sum_{i=1}^{N_A(t)} e(i,t)} = \overline{N_A(t)\{e(i,t)\}_A} = \overline{N_A^r(t)\{e(i,t)\}_A^r}, \tag{40}$$

$$\overline{D} = \sum_{i=1}^{N} \overline{M^A(i,t)d(i,t)} = \overline{\sum_{i=1}^{N_A(t)} d(iA,t)} = \overline{N_A(t)\{d(i,t)\}_A} = \overline{N_A^m(t)\{d(i,t)\}_A^m}. \tag{41}$$

It should be noted that, unlike their Lagrangian counterparts, Eulerian values of $E(t)$ and $D(t)$ are not necessarily equal.

In general, we can expect some correlations between the number of particles within *A* and the entrainment/disentrainment probability of each particle; for example, in relation to the so-called collective entrainment (e.g., Heyman et al., 2013, 2014). Again, we can simplify expressions under the condition of a large *A*, so that N_A, ${N_A}^m$, ${N_A}^r$ are (approximately) constant in time:

$$\overline{E} = \overline{\sum_{i=1}^{N_A(t)} e(i,t)} = N_A\overline{\{e(i,t)\}_A} = N_A^r\overline{\{e(i,t)\}_A^r}, \tag{42}$$

$$\overline{D} = \overline{\sum_{i=1}^{N_A(t)} d(i,t)} = N_A\overline{\{d(i,t)\}_A} = N_A^m\overline{\{d(i,t)\}_A^m}. \tag{43}$$

In the limit of large area, long time *T*, and stationary and ergodic process where we can assume that all trajectories have identical time averages, one obtains that $\overline{e} = 1/\langle\Delta t\rangle = 1/\tau$, with the result

$$[\overline{E}] = N_A[\overline{e}] = \frac{N_A}{\tau}. \tag{44}$$

4.3. Eulerian Variables: Sediment Discharge

For conditions of stationary and ergodic processes and a long period of observation *T*, the relationship between the sediment discharge and the Lagrangian variables is linked to relations that have already been derived (section 4.1). We have

$$\frac{[\lambda]}{T} = \frac{[J\langle\Delta x\rangle]}{[J\langle\Delta t\rangle]} = \frac{[\langle\Delta x\rangle]}{[\langle\Delta t\rangle]} = \frac{\xi}{\tau} \tag{45}$$

(note that *J* is constant under the above conditions). If we further consider a large area of observation, we obtain

$$\frac{[\overline{Q}]}{B} = w\frac{N_A}{A}\frac{[\lambda]}{T} = w\frac{N_A}{A}\frac{\xi}{\tau} = w\frac{N_A}{A}[\overline{e}]\xi = \frac{w}{A}[\overline{E}]\xi, \tag{46}$$

which is the typical Einstein-type formulation for sediment discharge. In equation (46) it is again expected that different kinds of averaging eventually result in the same values, under the assumptions considered above.

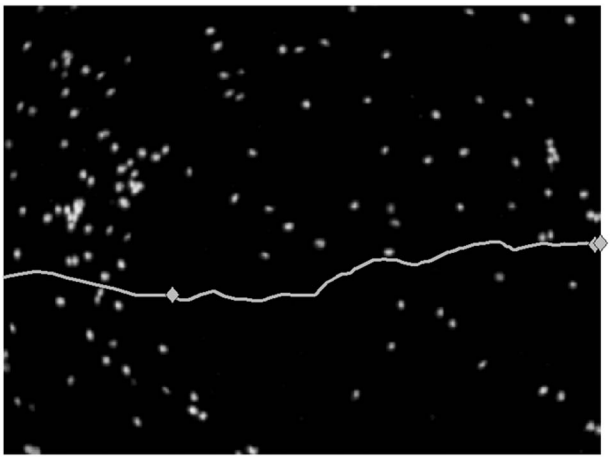

Figure 4. A movie frame covering the 273 × 200 mm^2 observation window with movable grains (white spots) and a sample particle track (white line). Motion is from left to right. Gray diamonds correspond to positions of rest along the path.

The two expressions for sediment discharge (equations (27) and (46)) are equivalent in this study under the general conditions discussed above (i.e., N_A is a constant resulting from a large area of observation, long period of observation, and stationary and ergodic processes).

5. Application to Experimental Results

5.1. Experimental Setup

The bed load transport experiments performed by Hosseini Sadabadi et al. (2016a) were conducted in a 5.5 m long pressurized duct with transparent walls and a cross section of 0.4 m × 0.11 m. Polybutylene-Terephthalate (PBT) grains with relative density equal to 1.27 and size of 3 mm were glued onto steel plates placed on the flume bottom to create a fixed rough bed. The standard deviation for the bed elevation was consistent with that measured for a movable bed composed of the same sediment (Campagnol et al., 2015).

The threshold flow velocity for sediment transport (U_c) was determined in preliminary experiments with a fully mobile bed and was equal to 0.23 m/s (Campagnol et al., 2013). During the same preliminary runs, a relationship between the flow velocity and the sediment transport capacity was determined.

The bed load run presented in this paper was obtained with a bulk flow velocity U = 0.32 m/s, resulting in U/U_c = 1.4. The shear velocity was calculated from the measured velocity profile. The corresponding Reynolds number based on the grain diameter was Re^* = 47, thus indicating a transitionally rough surface. Bed load particles identical to those in the fixed bed were fed at a constant rate at the upstream end of the duct. The sediment feeding rate was set equal to the transport capacity determined in the preliminary runs. However, as it will be shown, the disentrainment rate slightly exceeded the entrainment rate.

The use of a fixed bed obviously prevents some processes from being observed (for example, burial and reappearance of sediment particles). However, under weak transport conditions, the sediment transport is limited to a surficial layer of the bed and, therefore, a fixed bed may suffice to study the process. Specific comparisons performed by Campagnol et al. (2013, 2015) showed that properties of particle hops were not different in the two conditions, whereas a systematic comparison of rest times was not performed in those studies, which only considered motion events.

Particle motion was filmed (Hosseini Sadabadi et al., 2016a) from above at a rate of 32 fps, with an observation window of 273 mm in the streamwise direction and 200 mm in the transverse direction, and a filming duration of 50 s. Image processing enabled the bed load particles to be tracked. A flowchart of the measuring method was presented by Campagnol et al. (2013). The particles were first identified based on image thresholding and then tracked based on a criterion of minimum distance that was considered appropriate given a relatively limited concentration of white particles in the observation area (for a step-by-step description of the procedure applied to a similar experimental campaign, see a video article by Radice et al., 2017). Uncertainty in measurement of instantaneous particle velocity by this procedure was quantified by Campagnol et al. (2015), who also argued that a rate of 32 fps represented a satisfactory compromise between competing requirements of high temporal resolution and low uncertainty. Furthermore, a (time-consuming) manual validation and correction allowed the identification of particles during the entire time they spent in the observation window. The process generated 321 "global" trajectories, including periods of rest and movement for each particle. Assigning the instantaneous values of $M^m(i)$ to each particle required an operational criterion to decide if a particle was to be considered in motion or at rest at any time. Hosseini Sadabadi et al. (2016b) amended a rule proposed by Campagnol et al. (2013) and considered a particle to be in motion at a time instant if its x position at that time was larger than all the previous ones and smaller than all the following ones; otherwise, the particle was considered at rest at that time. Figure 4 shows a single frame of the movie, where the white spots correspond to movable grains, as the fixed grains constituting the bed were painted black. The path of a particle during the movie is superimposed onto the frame.

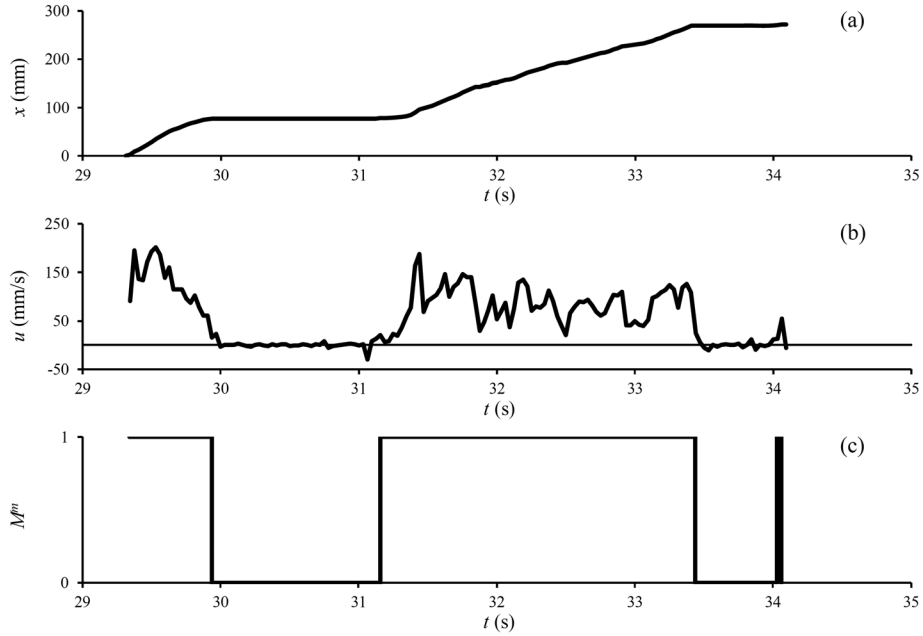

Figure 5. Lagrangian parameters [(a) position, (b) velocity, (c) clipping function for motion] for the particle whose track is shown in Figure 4.

Figure 5 shows the time series of the main Lagrangian parameters (x location, streamwise velocity component, and the clipping function for movement in Figures 5a, 5b, and 5c, respectively) for the trajectory shown in Figure 4. The particle crossed the whole observation window, so that the total measured displacement was equal to the window length. The particle entered the window at $t = 29.3$ s and left it at $t = 34.1$ s, so that the total time for which it was observed was only 4.8 s, much less than the movie duration (50 s). A new time variable, T_A, is therefore defined as the time that particle i has spent within the observation window:

$$T_A(i) = \int_t^{t+T} M_A(i,t)\mathrm{d}t = T\overline{M_A(i)} \tag{47}$$

The average value of T_A for the whole sample is 7.0 s, showing that the majority of particles spent only a short period of time within the observation area A.

Figure 6 shows the probability density function (PDF) of measured hop lengths, Δx. The distribution was determined using 680 hops that were obtained for the 321 tracked particles and has two peaks: the first peak is at $\Delta x = 0$ (most probable hops correspond to very small displacements), while the second is at $\Delta x = 270$ mm (corresponding to particles that crossed the whole window without stopping). The second peak represents truncated motions (hops longer than the measuring window); therefore, it results from all hops longer than 270 mm, rather than corresponding to a probability density at 270 mm.

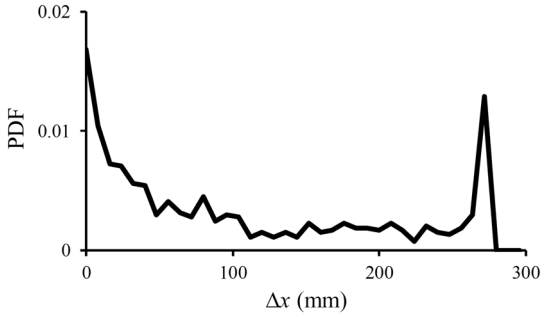

Figure 6. Probability density function of hop length.

The results discussed so far indicate that the observation window was relatively short compared to the particle hop lengths. This evidently limits the possibility of measuring Lagrangian quantities. On the other hand, no difficulties arise with Eulerian quantities. Figure 7 shows the time series of the total number of particles (moving + still) within the observation window, N_A, and the number of moving particles, $N_A{}^m$. While $N_A{}^m$ was stationary on average, N_A increased with time due to the previously mentioned imbalance between entrainment and disentrainment rates.

Finally, Figure 8 shows the time series of the instantaneous sediment flux, q, across a transverse line at $x = 73$ mm. The sediment flux corresponds to the sum of Dirac functions ($q = \Sigma_i \delta(t - t_0)$, equation (9)).

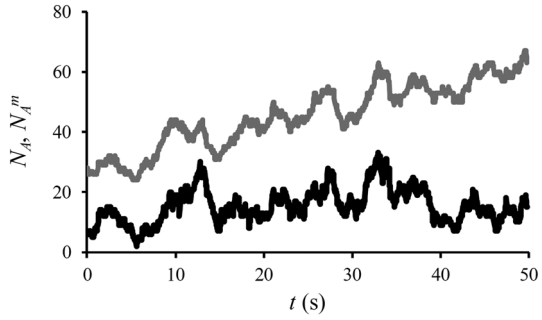

Figure 7. Temporal evolution of number of particles (gray) and number of moving particles (black) over A.

Therefore, its time series appears as a "bar code." The plot also includes the cumulative number of particle crossings within the duration of the experiment; the cumulative function progressively increases up to the total number of crossings N_Q = 260. Time series for entrainment and disentrainment functions (not shown) have a similar "bar code" appearance.

5.2. Lagrangian Proportion of Motion

The relative time of motion $\varphi_T{}^m(i)$ in the above experiments could not be computed from equation (15), because, due to the limitations of the observation window, each particle was observed only for a limited portion of the total time. A relative time of motion depending on the area of investigation was defined as: $\varphi_{TA}{}^m(i) = T_A{}^m(i)/T_A(i)$, where $T_A{}^m$ is the total time of movement for particle i during the period it spent within A. This $\varphi_{TA}{}^m$ was sketched together with $\varphi_T{}^m$ in Figure 3c. Figure 9 shows the PDF of $\varphi_{TA}{}^m$ for particles undergoing at least one hop during T. The plot indicates $\varphi_{TA}{}^m = 1$ as the most probable value, corresponding to particles that were never at rest within the measurement space-time window and thus providing another demonstration of the truncated particle motions already discussed on the basis of Figure 6.

The next task is to estimate the expected value ϑ^m for the proportion of motion. On the basis of the available data, neither $\varphi_T{}^m$ nor $\varphi_N{}^m$ could be computed by their respective definitions (equations (15) and (16)) because the particles were within the observation area for a limited time. Therefore, the global proportion of motion was estimated by pooling all the observed particles. Using this approach, one envisions each particle observation as a random outcome of the same process, as discussed by Heyman et al. (2016). Therefore, the global proportion of motion was estimated using a new version of equation (15) that jointly considered the contributions of all the observed particles to a global T^m and a global T:

$$\vartheta^m \cong \frac{\sum_{i=1}^{N} T_A^m(i)}{\sum_{i=1}^{N} T_A(i)} \tag{48}$$

A value of ϑ^m = 0.340 was obtained, indicating that under the applied hydrodynamic conditions (U/U_c = 1.4), the intermittency of the sediment transport process resulted in a 35% proportion of motion and a 65% proportion of stillness.

5.3. Eulerian Proportion of Motion

Figure 10 shows the time series of the Eulerian relative number of moving particles within the observation window, $\varphi_A{}^m(t)$. Its time average is 0.342, which is very similar to the relative time of motion obtained from (48). As discussed in section 3.2, this result is to be expected for large numbers of particles within the observation area, as a consequence of N_A and $\varphi_A{}^m$ being independent of time. Instead, it is clear from Figures 7 and 10 that such a condition is not met for the present data set. Nevertheless, the Lagrangian and Eulerian proportions of motion are in good agreement: $\{\varphi_T^m\} \cong \overline{\varphi_A^m(t)}$ with a 0.5% difference, thanks to the method of considering tracks jointly by means of equation (48).

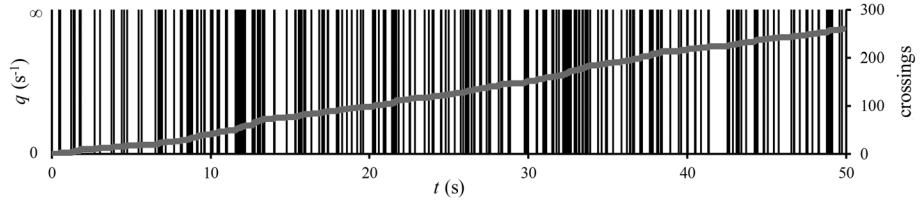

Figure 8. Time series of instantaneous sediment flux across a transverse line, corresponding to a sum of delta functions at particle crossings (black, left axis) and cumulative number of crossings (gray, right axis).

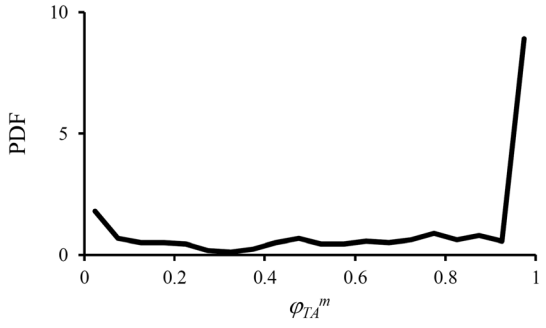

Figure 9. Probability density function of $\varphi_{TA}{}^m(i)$.

The correlation between the fluctuating terms of N_A and $\varphi_A{}^m$ is now explored. A comparison of different averaging options demonstrates that the correlation was weak for the present experiment:

$$\overline{N_A^m} = \overline{N_A \varphi_A^m} = 15.40 \cong \overline{N_A}\,\overline{\varphi_A^m} = 45.42 \times 0.342 = 15.55 \tag{49a}$$

$$\overline{N_A{}'\{M^m\}_A{}'} = -0.15 \tag{49b}$$

Some arguments about how this result may change with the size of the observation area are provided in section 6. Furthermore, it should be noted that the present experiment involved weak bed load over a plane fixed bed. Different bed conditions and transport intensities (particularly those higher than described here) may change the active processes and, in turn, the correlation terms. For example, processes such as sediment burial and reappearance in a mobile layer (possibly, in the presence of bedforms) may strongly alter the temporal fluctuations with respect to those for continuously exposed particles (see, e.g., Ghilardi et al., 2014a, 2014b; Iwasaki et al., 2017; Voepel et al., 2013). Threshold sizes to consider spatial and temporal scales large enough to achieve process uniformity/stationarity are expected to be more demanding than in the present case.

5.4. Persistence of Motion

As mentioned above, limited size of the space-time observation window may prevent a sound estimation of the properties of hops. The examples given in Figures 6 and 9 demonstrate that several hops are longer than 270 mm, but we cannot know how long they are. Some discussion of how to handle effects from truncation by the observation window is provided in Fathel et al. (2015). As a matter of fact, measured PDFs are strongly distorted, so that they do not allow derivation of any statistics for Δx, nor for Δt (not even mean values). For example, as we cannot disregard truncation of hops, it is not possible to use equations (30) to (33) to calculate mean values for event duration or entrainment/disentrainment functions. However, in this case, one can also consider the tracks jointly, as was done in equation (48):

$$\tau^m \cong \frac{\sum_{i=1}^{N} T_A^m(i)}{\sum_{i=1}^{N} J_A(i)} \tag{50}$$

where J_A is the number of events observed for one particle within A, keeping in mind that $J_A = 0$ for particles that do not stop. Equation (50) thus calculates the average duration of motion by dividing the total observed time of motion of all particles and all motion events measured within the observation window by the total number of such events. This method is similar to some developments proposed by Heyman et al. (2016, p. 12 of supporting information), who evaluated a first moment of a particle deposition rate "dividing the number of deposition events by the cumulative time of travel by particles." In a system at equilibrium, the number of entrainment and deposition events is the same. However, as previously discussed, the system was not really stationary in the experiment described here, so that the numbers of entrainment and disentrainment events were not exactly the same (specifically, we observed 376 entrainment and 412 disentrainment events). For this application, we simply use the mean between the two values, thus obtaining

$$\begin{aligned} \tau &= 5.73 \text{ s} \\ \tau^m &= 1.95 \text{ s} \\ \tau^r &= 3.76 \text{ s} \end{aligned} \tag{51}$$

Given the way in which values for τ were calculated, the estimate of ϑ^m based on the duration of motion yields results identical to those of section 5.3: $\tau^m/\tau = \vartheta^m = 0.340$. The expected value of the hop length, ξ, is estimated by applying the method of equation (50) to traveled distances and hop lengths as

$$\xi \cong \frac{\sum_{i=1}^{N} \lambda_A(i)}{\sum_{i=1}^{N} J_A(i)} \tag{52}$$

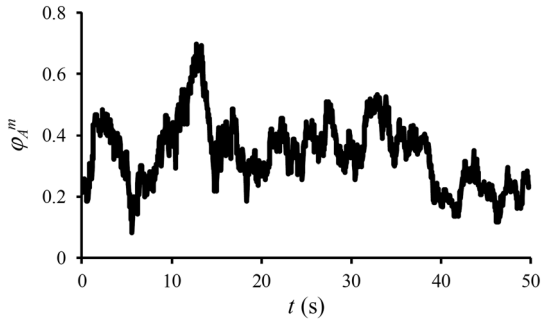

Figure 10. Temporal evolution of the relative number of moving particles within A.

where λ_A is the total distance traveled by a particle while it was within A (which is the spatial counterpart of ${T_A}^m$ in equation (50)).

Finally, expected values for sediment velocity (indicating the effective velocity with v and the velocity during motion with v^m) can be computed by considering the estimated hop length and T or T^m, respectively. Resulting values are

$$\begin{aligned} \xi &= 177 \ \text{mm} \\ v &= \frac{\xi}{\tau} = 30.3 \ \text{mm/s} \\ v^m &= \frac{\xi}{\tau^m} = 89.1 \ \text{mm/s} \end{aligned} \tag{53}$$

Note that the mean value derived from the PDF in Figure 6 is $\langle \Delta x \rangle$ = 102 mm, demonstrating that truncation produces a strong underestimation for the mean value of the hop length if the latter is estimated as the mean of the PDF of measured hops. An analogous conclusion can be derived for motion time ($\langle \Delta t^m \rangle$ = 1.18 s) and resting time ($\langle \Delta t^r \rangle$ = 3.34 s) when directly derived as averages of the measured truncated sample. These results highlight the need to reconsider how mean values for Lagrangian properties have been determined in earlier studies.

5.5. Sediment Discharge

Particle crossings corresponding to instantaneous sediment discharge are shown in Figure 8. The time average of the sediment discharge can be evaluated directly from the total number of particles crossing the reference target within the duration of the movie (N_Q = 260):

$$\frac{\overline{Q}}{w} = \frac{N_Q}{T} = 5.2 \, \text{crossings/s} \tag{54}$$

An independent mixed Eulerian/Lagrangian evaluation stems from equations (27) and (46):

$$\frac{\overline{Q}}{w} = B \frac{\overline{N_A}}{A} \frac{\xi}{\tau} = 5.1 \, \text{crossings/s} \tag{55}$$

thus proving the consistency of the estimates for the various kinematic quantities. The latter relationships yield a remarkable argument that average values of hop properties (which are Lagrangian quantities suffering from a significant bias due to the observation window) can be obtained from purely Eulerian measurements of Q (or alternatively N_A and u based on equation (27)) and E, thus bypassing the already mentioned practical impossibility of obtaining rigorously Lagrangian measurements of particle motion. In other words, measurements of Lagrangian variables can be hindered by the limited spatial and temporal scales of measurement, while these conditions are more compatible with measurements of Eulerian quantities. It is therefore useful to link Lagrangian and Eulerian statistics of processes, because the latter may allow one to infer characteristics of the former.

6. Discussion

The conceptual framework presented in this work considers bed load particles individually and attributes all their properties to their center of mass (concentrated particles). From a Lagrangian perspective, everything is represented by the temporal history of one particle, and mean values can be obtained by time, sample or event averaging. Eulerian variables are defined by averaging over a control volume and can be further averaged in time. Crucial for the framework is the introduction of two clipping functions representing, at any given time, (i) if one particle is in motion or at rest and (ii) if one particle is within an area of observation.

The identification of particle entrainment and disentrainment is necessary to derive all the quantities related to these events (entrainment and disentrainment functions, hop properties). This requires operational criteria to be applied to the measured particle tracks for assigning the instantaneous value of M^m. As described above, a criterion based on particle position was used in this work. Operational criteria for labeling the particle motion state can also consider different quantities. Among recent examples, Seizilles et al. (2014) considered the ratio of the standard deviation of particle position over four successive frames to the particle size. Heyman et al. (2016) used a two-parameter criterion based on particle velocity and elevation above the

bed. In addition, Hosseini Sadabadi et al. (2016b) presented a sensitivity analysis of some investigated quantities to the criterion used to recognize particle motion or rest, comparing the proposed criterion to the one of Campagnol et al. (2013). The criterion of Hosseini Sadabadi et al. (2016b), more restrictive than that of Campagnol et al. (2013), returned, for the same experiment, a different number of hops (that were 3 times less); the frequency of occurrence of relatively shorter and longer hops was different, resulting, for the new criterion, in larger mean values for hop length and duration. This sensitivity could be further extended to other types of criteria and represents a challenge for quantification of some key properties of sediment transport. However, this issue has not been examined in the present work, which has, instead, focused on the conceptual framework for analysis.

A Lagrangian analysis requires individual particles to be followed. This is not necessary with an Eulerian standpoint, which considers the quantity of sediment within, for example, some reference volume. Our framework requires a base sample of N particles to be defined; the sample is necessary to provide deterministic links between the two approaches (see, e.g., equation (5) and similar ones with sums over particles). The only requirement that we imposed on the sample was that all the particles were identical, although this requirement can be removed by accounting for the specific volume of each particle. Statistical properties of our analysis may be influenced by small sample sizes, but otherwise are not sample dependent. However, different quantities can be defined depending on how the initial sample of particles is chosen. A significant example is represented by the proportion of motion introduced in this work. The relative number of moving particles expressed by equation (21) is analogous to other descriptors that are present in the literature; for example, the particle concentration used by Radice et al. (2009) or the different versions of particle activity used by Roseberry et al. (2012) and Heyman et al. (2014). However, the different values obtained according to how the initial sample of particles is chosen can be retrieved from each other using appropriate scaling factors.

The definitions presented in our analysis are general and do not require specific hypotheses. Instead, particular conditions may be needed to neglect, for example, correlation effects. A specific and particularly relevant issue is the size of the area of observation. Absolute bounds for classifying an area as large or small cannot be given based on a single experiment. Consequently, they fall outside of the scope of this paper. However, some discussion in this regard is provided as follows.

On a phenomenological basis, one can consider that the size of a reference area, A, influences how quantities vary or covary. For example, Heyman et al. (2014) studied the spatial correlation functions of particle activity in the bed load transport. Furthermore, Radice et al. (2009) analyzed the bed load particle concentration and showed that its variance decreased for increasing A, following a power law. A similar finding was reported by Roseberry et al. (2012). An analogous exercise can be attempted for the correlation introduced in equation (24). For the area used in the experiment documented here (equal to 6,000 times the squared particle size), the weight of the correlation terms was as low as 1%, as shown in equations (49a) and (49b). Reduced areas of observation, corresponding to 1,100, 280, and 45 times the squared particle size, produced weights of the correlation term of 4, 7, and 9%, respectively. One could conclude that, for this aspect, the area used in this experiment was sufficiently "large" because 1% is sufficiently "small." However, assigning thresholds is never exempt from some degree of arbitrariness.

On the other hand, the area of observation was too small for quantification of the Lagrangian properties. This was shown by PDFs in Figures 6 and 9, making it impossible to apply equations (15) and (16) to compute the Lagrangian proportion of motion, equations (30) to (33) for the hop duration, and equations (35) and (36) for the hop length. We pooled the particle tracks into a single sample and applied equations (48), (50), and (52) to compute these properties. Track pooling can be performed in two alternative ways, with counterparts of equations (48), (50), and (52) being

$$\vartheta^m \cong \frac{1}{N}\sum_{i=1}^{N}\frac{T_A^m(i)}{T_A(i)} \tag{56}$$

$$\tau^m \cong \frac{1}{N}\sum_{i=1}^{N}\frac{T_A^m(i)}{J_A(i)} \tag{57}$$

$$\xi \cong \frac{1}{N}\sum_{i=1}^{N}\frac{\lambda_A(i)}{J_A(i)} \tag{58}$$

The difference between the set of equations (48)–(50)–(52) and the set of (56)–(57) and (58) is that, in the former case, summation is performed for both the numerator and denominator of a considered ratio, while in the latter case it is performed for the ratio, so that the order of the operations (ratio and summation) is inverted. For the case of a large area, the homologous formulae will return the same values. Instead, for a small area, equation (56) does not perform as well as (48) because it neglects the correlation (introduced by the limited area of observation) between the time that a particle spends within A and the time that the particle spends in motion within A. Instead, one needs to find the average of the function M^m over the domain that consists of all time intervals that any particle spent within the reference area A. With reference to Figure 3b, this averaging domain consists of all rectangles plotted with thick black lines, an approach that leads to equation (56). For equations (57) and (58), the explanation is different: a limited area of observation introduces particles that do not stop, for which $J_A = 0$, so that the ratios involved in these equations would not have a finite value.

7. Conclusions

Similar to many other physical processes, bed load transport can be described by taking either a Lagrangian approach (following the motion of individual particles) or an Eulerian approach (observing grain motion at prescribed locations). Various attempts to represent the kinematics of the process have appeared in recent years in the literature, frequently with extensive use made of statistical tools in consideration of the fluctuating nature of bed load.

The unifying framework proposed in this study for analysis of the sediment transport process merged the Lagrangian and Eulerian views and included all the quantities most typically used to formulate sediment transport models. The intermittency of the sediment transport process was associated with two complementary concepts: (i) proportion of motion and (ii) persistence of motion. The Lagrangian representations of the proportion of motion were a relative time of motion for single particles and a number of particles in motion relative to the full particle sample. The Eulerian indicator was the relative number of particles in motion over a certain area of the bed. The persistence of motion was related to the successions of particle entrainment and disentrainment events that are needed to determine the properties of particle hops. Starting from particle tracks, and through the definition of appropriate clipping functions for particle motion and for particles being above a certain reference area of observation, several mean quantities could be obtained: for example, particle concentration, hop length and duration, time of rest, entrainment and disentrainment fluxes, and sediment transport rate. The presented set of equations, therefore, enabled key averaged quantities to be derived from the kinematics of individual grains and provided a unifying framework for relating Lagrangian and Eulerian approaches, thereby addressing the goals of our study.

The framework for analysis proposed in this paper involved only first moments of quantities. In fact, correlation effects can be discarded if one uses a large observation area as support for the conceptualization of the process. However, the estimation of mean Lagrangian properties (e.g., hop length) requires an area larger than a threshold area to make spatial and temporal correlations vanish. One can first use track pooling to obtain mean values for Lagrangian quantities. Additionally, the framework proposed in this study demonstrated that it is possible to obtain the mean values for Lagrangian properties of particle hops from Eulerian quantities, whose reliable determination is not prevented by the size of an observation area. In fact, the mean hop length can be obtained from Eulerian data of sediment transport rate and entrainment flux. In this way, the research presented in this paper strongly supports laboratory or field investigations devoted to the measurement of mean particle hops.

The definitions and relationships outlined in this study constitute a (relatively) simple framework for analysis, whose self-consistency is ensured by the fact that all the quantities are deterministically linked to the motion of individual grains via the two clipping functions. When applied to experimental data, the framework has demonstrated its usefulness in clarifying limitations of the laboratory setup with respect to the different descriptions of motion, and it enabled operational solutions to be applied. We expect this set of definitions to be valuable for achieving parameterization of the descriptors of sediment kinematics.

Appendix A: Expected Value of Time-Averaged Volumetric Sediment Discharge Across a Target Surface

Consider a set of identical candidate particles that can potentially contribute to volumetric discharge, $\overline{Q}$, across a target surface during the observation period of duration T ($t_1 < t \le t_1 + T$). At the beginning of the observation window, at $t = t_1$, the candidate particles are located upstream from the target (white particles in Figure A1a), and it is assumed that they travel only in the positive x direction.

Furthermore, the spatial distribution of the particles over the area of observation, A, is uniform in the sense that the total number of particles per unit plan area N_A/A does not change in space. For this condition to be met, the plan area has to be sufficiently large to provide a stable value of N_A/A as A moves in space.

During the observation period, all candidate particles travel some distance $\underline{\lambda} \ge 0$ (Figure A1a). For some of them, the distance will exceed the particle's original distance from the target (black circles), and for some of them it will not (gray circles). The total number of particles that cross the target, and therefore contribute to the discharge, is denoted with N_Q.

We assume that the PDF for a candidate particle to travel a distance during the observation window T is known, and identical for all particles. From this known PDF, it is possible to express the exceedance probability function P, such that it is equal to the probability of λ being equal to or exceeding a set of its possible values, $\underline{\lambda}$: $P(\underline{\lambda}) = P(\lambda \ge \underline{\lambda})$. A typical shape of $P(\underline{\lambda})$ is shown in Figure A1c. Since $\underline{\lambda}$ is always greater or equal to zero, $P(\underline{\lambda})$ has the following properties:

$$P(0) = P(\lambda \ge 0) = 1, \tag{A1}$$

and

$$\int_0^\infty P(\underline{\lambda})\ \mathrm{d}\underline{\lambda} = [\lambda]. \tag{A2}$$

Equation (A2) requires the probability distribution of λ to be thin tailed, as discussed, for example, by Furbish, Roseberry, et al. (2012). We now compare the distances of the candidate particles from the target, ℓ, and the

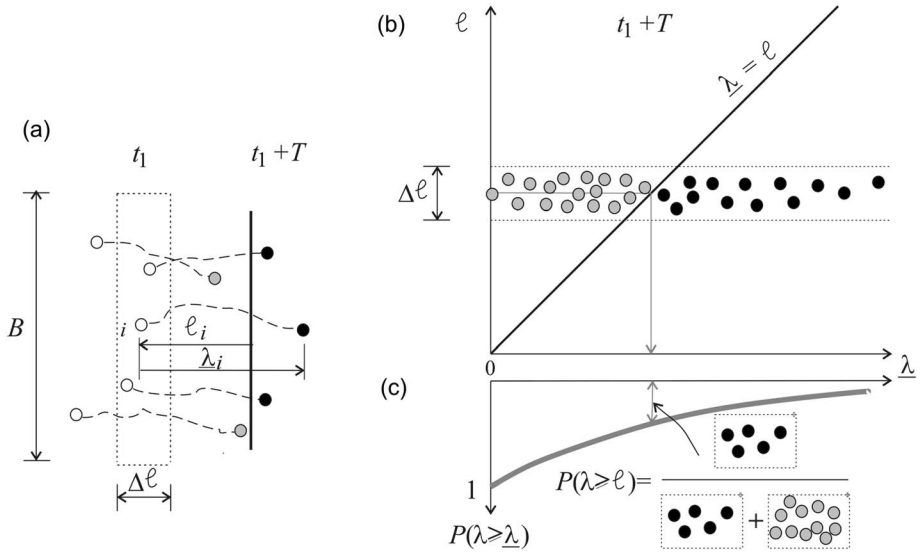

Figure A1. (a) Definition sketch which shows a set of particles and a target surface (thick line). White circles show the position of the candidate particles at $t = t_1$. They are all located upstream from the target surface, at various distances $\ell_i (i = 1, 2 \ldots)$. During an observation period T the candidate particles travel distances $\underline{\lambda}_i$. Particles for which $\underline{\lambda}_i \ge \ell_i$ contribute to the sediment discharge across the target during the observation period T; (b) position of some candidate particles at $t_1 + T$ in the coordinate system $(\underline{\lambda}, \ell)$. These particles originate from a narrow strip (width $\Delta\ell$, shown with dotted lines in both (a) and (b)), located at a distance $\ell \pm \Delta\ell/2$ from the target surface. Gray particles have traveled distances less than ℓ, whereas black particles have traveled distances that are equal to or larger than ℓ, so they have contributed to sediment discharge; (c) probability that the distance traveled by a particle is equal to or larger than $\underline{\lambda}$. The value corresponding to $\underline{\lambda} = \ell$ is the ratio of the expected number of black particles and the total number of particles.

distances they travel during time T, $\underline{\lambda}$. It is convenient to do this in the coordinate system $(\underline{\lambda}, \ell)$ shown in Figure A1b, which also shows the line $\underline{\lambda} = \ell$. Consider a very short strip, $\Delta\ell$, centered at an arbitrary distance, ℓ, from the target surface. The total number of candidate particles contained within the strip is $\frac{N_A}{A} B\Delta\ell$, where B is the width of the target surface. The percentage of the particles from this strip expected to travel a distance equal to or larger than ℓ (i.e., that travel across the line $\underline{\lambda} = \ell$, black circles in Figure A1b) and hence contribute to the discharge across the target, is equal to the corresponding probability $P(\lambda \geq \underline{\lambda} = \ell) = P(\underline{\lambda}) = P(\ell)$, shown in Figure A1c. The expected total number of the candidate particles from the strip $\Delta\ell$ that contribute to the discharge is therefore equal to $\frac{N_A}{A} B \ \Delta\ell \ P(\underline{\ell})$. Allowing the length of the strip to become infinitely small ($\Delta\ell \rightarrow d\underline{\ell}$) and integrating along the entire length upstream from the target surface yields the expected number of particles that contribute to the discharge during the period T:

$$[N_Q] = \frac{N_A}{A} B \int_0^\infty P(\ell) \ d\ell = \frac{N_A}{A} B[\lambda] \tag{A3}$$

The time-averaged sediment discharge during the observation period T is equal to the volume of particles (wN_Q, where w is the volume of each particle), divided by T. The expected average sediment discharge during the period T is therefore equal to

$$[\overline{Q}] = w \frac{N_A}{A} B \frac{[\lambda]}{T} \tag{A4}$$

Notation

Indices and coordinates.

i	index for particles
j	index for events
t	time coordinate
x	streamwise coordinate
y	transverse coordinate

Reference times and locations.

t_0	time at which a particle reaches a target line
x_0	location of a target line

Domain size.

A	reference bed area
J	number of events for one particle
J_A	number of events observed for one particle within A
L	streamwise extension of A
N	number of particles in the sample
N_A	number of particles within A
T	total time of Lagrangian observation
T_A	time that a particle spends within A

Averaging options for a generic θ variable.

$\langle\theta\rangle$	average over particle events
$\overline{\theta}$	average over time
θ'	deviation from a temporal mean
$\{\theta\}$	average over particles
$\{\theta\}_A$	average over particles within A
$\{\theta\}_A^m$	average over moving particles within A

$\{\theta\}_A^r$ average over particles resting within A
$[\theta]$ expected value
P probability

Clipping functions for particle states.
M^A clipping function for particle within A
M^m clipping function for particle motion

Mathematical functions.
H Heaviside function
δ Dirac function

Expected values.
ϑ^m expected value of proportion of motion
τ $\tau^m + \tau^r$, expected value of Δt
τ^m expected value of Δt^m
τ^r expected value of Δt^r
υ expected value of u
υ^m expected value of u^m
ξ expected value of Δx

Physical properties.
B width of a target line
C $w\, N_A/A$, concentration of particles within A
D Eulerian disentrainment function
d Lagrangian disentrainment function
E Eulerian entrainment function
e Lagrangian entrainment function
ℓ particle distance from a target line
N_A^m number of moving particles within A
N_A^r number of particles resting within A
N_Q number of particles crossing a target line
N^m number of moving particles
q crossing function
Q sediment transport rate
Re^* friction Reynolds number
T_A^m time that a particle spends in motion within A
t^d instant of particle disentrainment
t^e instant of particle entrainment
T^m total time of motion for one particle
T^r total time of rest for one particle
U bulk flow velocity
u instantaneous particle velocity
U_c threshold flow velocity for sediment transport
u^m instantaneous particle velocity (for motion state)
$u_{\Delta x}$ average effective particle velocity within a hop
$u_{\Delta x}^m$ average particle velocity within a hop
V volume of particles crossing a target line
w particle volume
w_A volume of particles within A
$\Delta\ell$ streamwise length of a narrow strip of bed
Δt duration of a particle event (motion+stillness)

Δt^m	duration of a motion event
Δt^r	duration of a stillness event
Δw_A	change of w_A
Δx	length of particle motion (or hop length, or displacement in a motion event)
${\varphi_A}^m$	Eulerian relative number of particles in motion
${\varphi_N}^m$	Lagrangian relative number of particles in motion
${\varphi_{TA}}^m$	relative time of motion for a particle, for the duration of its stay within A
${\varphi_T}^m$	Lagrangian relative time of motion
λ	distance traveled by a particle within T
λ_A	observed travel distance for a particle within A
θ	any quantity

Acknowledgments
The research reported in this paper was partially supported by the Research Executive Agency, through the 7th Framework Programme of the European Union, Support for Training and Career Development of Researchers (Marie Curie-FP7-PEOPLE-2012-ITN), which funded the Initial Training Network (ITN) HYTECH "Hydrodynamic Transport in Ecologically Critical Heterogeneous Interfaces", N.316546. The second author was supported by the UK's Engineering and Physical Sciences Research Council (grant EP/K013513/1). The authors wish to thank Andrea Marion and Andrea Bottacin Busolin for stimulating discussions on the definition framework, and John Buffington for handling the manuscript submission and for the extreme care put into the manuscript editing. Christophe Ancey, David Furbish, Joris Heyman, and PhD student Gauthier Rousseau provided thought-provoking comments, thanks to which the manuscript was considerably improved. Data are available from the institutional web site of the Politecnico di Milano at http://intranet.dica.polimi.it/people/radice-alessio/.

References

Ancey, C. (2010). Stochastic modeling in sediment dynamics: Exner equation for planar bed incipient bed load transport conditions. *Journal of Geophysical Research*, *115*, F00A11. https://doi.org/10.1029/2009JF001260

Ancey, C., Bigillon, F., Frey, P., Lanier, J., & Ducret, R. (2002). Saltating motion of a bead in a rapid water stream. *Physical Review E*, *66*(3), 036306. https://doi.org/10.1103/PhysRevE.66.036306

Ancey, C., Böhm, T., Jodeau, M., & Frey, P. (2006). Statistical description of sediment transport experiments. *Physical Review E*, *74*(1), 011302. https://doi.org/10.1103/PhysRevE.74.011302

Ancey, C., Davison, A. C., Böhm, T., Jodeau, M., & Frey, P. (2008). Entrainment and motion of coarse particles in a shallow water stream down a steep slope. *Journal of Fluid Mechanics*, *595*, 83–114. https://doi.org/10.1017/S0022112007008774

Ancey, C., & Heyman, J. (2014). A microstructural approach to bed load transport: Mean behaviour and fluctuations of particle transport rates. *Journal of Fluid Mechanics*, *744*, 129–168. https://doi.org/10.1017/jfm.2014.74

Ballio, F., Nikora, V., & Coleman, S. E. (2014). On the definition of solid discharge in hydro-environment research and applications. *Journal of Hydraulic Research*, *52*(2), 173–184. https://doi.org/10.1080/00221686.2013.869267

Berzi, D., Jenkins, J. T., & Valance, A. (2015). Periodic saltation over hydrodynamically rough beds: Aeolian to aquatic. *Journal of Fluid Mechanics*, *786*, 190–209. https://doi.org/10.1017/jfm.2015.601

Blom, A., & Parker, G. (2004). Vertical sorting and the morphodynamics of bed form-dominated rivers: A modeling framework. *Journal of Geophysical Research*, *109*, F02007. https://doi.org/10.1029/2003JF000069

Böhm, T., Ancey, C., Frey, P., Roboud, J., & Ducottet, C. (2004). Fluctuations of the solid discharge of gravity-driven particle flows in a turbulent stream. *Physical Review E*, *69*(6), 061307. https://doi.org/10.1103/PhysRevE.69.061307

Bunte, K., & Abt, S. R. (2005). Effect of sampling time on measured gravel bed load transport rates in a coarse-bedded stream. *Water Resources Research*, *41*, W11405. https://doi.org/10.1029/2004WR003880

Campagnol, J., Radice, A., & Ballio, F. (2012). Scale-based statistical analysis of sediment fluxes. *Acta Geophysica*, *60*(6), 1744–1777. https://doi.org/10.2478/s11600-012-0028-6

Campagnol, J., Radice, A., Ballio, F., & Nikora, V. (2015). Particle motion and diffusion at weak bed load: Accounting for unsteadiness effects of entrainment and disentrainment. *Journal of Hydraulic Research*, *53*(5), 633–648. https://doi.org/10.1080/00221686.2015.1085920

Campagnol, J., Radice, A., Nokes, R., Bulankina, V., Lescova, A., & Ballio, F. (2013). Lagrangian analysis of bed-load sediment motion: Database contribution. *Journal of Hydraulic Research*, *51*(5), 589–596. https://doi.org/10.1080/00221686.2013.812152

Cao, Z. (1997). Turbulent bursting-based sediment entrainment function. *Journal of Hydraulic Engineering*, *123*(3), 233–236. https://doi.org/10.1061/(ASCE)0733-9429(1997)123:3(233)

Charru, F., Mouilleron, H., & Eiff, O. (2004). Erosion and deposition of particles on a bed sheared by a viscous flow. *Journal of Fluid Mechanics*, *519*, 55–80. https://doi.org/10.1017/S0022112004001028

Cohen, H., Laronne, J. B., & Reid, I. (2010). Simplicity and complexity of bed load response during flash floods in a gravel bed ephemeral river: A 10 year field study. *Water Resources Research*, *46*, W11542. https://doi.org/10.1029/2010WR009160

Coleman, S. E., & Nikora, V. I. (2009). Exner equation: A continuum approximation of a discrete granular system. *Water Resources Research*, *45*, W09421. https://doi.org/10.1029/2008WR007604

Einstein, H. A. (1937). *Der Geschiebebetrieb als Wahrscheinlichkeitsproblem*, Verlag Rascher, Zurich. (Engl. trans.: in: H. Shen (Ed.), 1972. Sedimentation Symposium to Honor H. A. Einstein, H.W. Shen, Fort Collins, CO).

Fan, N., Singh, A., Guala, M., Foufoula-Georgiou, E., & Wu, B. (2016). Exploring a semimechanistic episodic Langevin model for bed load transport: Emergence of normal and anomalous advection and diffusion regimes. *Water Resources Research*, *52*, 2789–2801. https://doi.org/10.1002/2015WR018023

Fan, N., Zhong, D., Wu, B., Foufoula-Georgiou, E., & Guala, M. (2014). A mechanistic-stochastic formulation of bed load particle motions: From individual particle forces to the Fokker-Planck equation under low transport rates. *Journal of Geophysical Research: Earth Surface*, *119*, 464–482. https://doi.org/10.1002/2013JF002823

Fathel, S. L., Furbish, D. J., & Schmeeckle, M. W. (2015). Experimental evidence of statistical ensemble behavior in bed load sediment transport. *Journal of Geophysical Research: Earth Surface*, *120*, 2298–2317. https://doi.org/10.1002/2015JF003552

Fathel, S., Furbish, D., & Schmeeckle, M. (2016). Parsing anomalous versus normal diffusive behavior of bedload sediment particles. *Earth Surface Processes and Landforms*, *41*(12), 1797–1803. https://doi.org/10.1002/esp.3994

Frey, P., Ducottet, C., & Jay, J. (2003). Fluctuations of bed load solid discharge and grain size distribution on steep slopes with image analysis. *Experiments in Fluids*, *35*(6), 589–597. https://doi.org/10.1007/s00348-003-0707-9

Furbish, D. J., Haff, P. K., Roseberry, J. C., & Schmeeckle, M. W. (2012). A probabilistic description of the bed load sediment flux: 1. Theory. *Journal of Geophysical Research*, *117*, F03031. https://doi.org/10.1029/2012JF002352

Furbish, D. J., Roseberry, J. C., & Schmeeckle, M. W. (2012). A probabilistic description of the bed load sediment flux: 3. The particle velocity distribution and the diffusive flux. *Journal of Geophysical Research*, *117*, F03033. https://doi.org/10.1029/2012JF002355

Ganti, V., Singh, A., Passalacqua, P., & Foufoula-Georgiou, E. (2009). Subordinated Brownian motion model for sediment transport. *Physical Review E*, *80*(1), 011111. https://doi.org/10.1103/PhysRevE.80.011111

Garcia, M. H. (2008). Sediment transport and morphodynamics. In M. H. Garcia (Ed.), *Sedimentation Engineering: Processes, Measurements, Modeling, and Practice*, *American Society of Civil Engineers, Manuals and Reports on Engineering Practice* (Vol. 110, pp. 21–164). Reston, USA: ASCE. https://doi.org/10.1061/9780784408148.ch02

Garcia, C., Cohen, H., Reid, I., Rovira, A., Úbeda, X., & Laronne, J. B. (2007). Processes of initiation of motion leading to bedload transport in gravel-bed rivers. *Geophysical Research Letters*, *34*, L06403. https://doi.org/10.1029/2006GL028865

Ghilardi, T., Franca, M. J., & Schleiss, A. J. (2014a). Bed load fluctuations in a steep channel. *Water Resources Research*, *50*, 6557–6576. https://doi.org/10.1002/2013WR014449

Ghilardi, T., Franca, M. J., & Schleiss, A. J. (2014b). Period and amplitude of bedload pulses in a macro-rough channel. *Geomorphology*, *221*, 95–103. https://doi.org/10.1016/j.geomorph.2014.06.006

Hassan, M. A., Voepel, H., Schumer, R., Parker, G., & Fraccarollo, L. (2013). Displacement characteristics of coarse fluvial bed sediment. *Journal of Geophysical Research: Earth Surface*, *118*, 155–165. https://doi.org/10.1029/2012JF002374

Heays, K. G., Friedrich, H., Melville, B. W., & Nokes, R. (2014). Quantifying the dynamic evolution of graded gravel beds using particle tracking velocimetry. *Journal of Hydraulic Engineering*, *140*(7), 04014027. https://doi.org/10.1061/(ASCE)HY.1943-7900.0000850

Heyman, J., Bohorquez, P., & Ancey, C. (2016). Entrainment, motion and deposition of coarse particles transported by water over a sloping mobile bed. *Journal of Geophysical Research: Earth Surface*, *121*, 1931–1952. https://doi.org/10.1002/2015JF003672

Heyman, J., Ma, H. B., Mettra, F., & Ancey, C. (2014). Spatial correlations in bed load transport: Evidence, importance, and modeling. *Journal of Geophysical Research: Earth Surface*, *119*, 1751–1767. https://doi.org/10.1002/2013JF003003

Heyman, J., Mettra, F., Ma, H. B., & Ancey, C. (2013). Statistics of bedload transport over steep slopes: Separation of time scales and collective motion. *Geophysical Research Letters*, *40*, 128–133. https://doi.org/10.1029/2012GL054280

Hosseini Sadabadi, S. A., Radice, A., & Ballio, F. (2016a). An analysis of entrainment and deposition rate fluctuations in weak bed load transport. In P. M. Rowiński & A. Marion (Eds.), *Hydrodynamic and Mass Transport at Freshwater Aquatic Interfaces*, *GeoPlanet: Earth and Planetary Sciences* (pp. 333–342). Berlin: Springer.

Hosseini Sadabadi S. A., Radice, A., & Ballio, F. (2016b). Post-processing of particle tracking data for phenomenological description of weak bed-load sediment transport, Proc. River Flow 2016, VIII International Conference on Fluvial Hydraulics, St. Louis, US.

Hu, C., & Hui, Y. (1996). Bed-load transport. I: Mechanical characteristics. *Journal of Hydraulic Engineering*, *122*(5), 245–254. https://doi.org/10.1061/(ASCE)0733-9429(1996)122:5(245)

Iwasaki, T., Nelson, J., Shimizu, Y., & Parker, G. (2017). Numerical simulation of large-scale bed load particle tracer advection-dispersion in rivers with free bars. *Journal of Geophysical Research: Earth Surface*, *122*, 847–874. https://doi.org/10.1002/2016JF003951

Kempe, T., & Fröhlich, J. (2012). Collision modelling for the interface-resolved simulation of spherical particles in viscous fluids. *Journal of Fluid Mechanics*, *709*, 445–489. https://doi.org/10.1017/jfm.2012.343

Lajeunesse, E., Malverti, L., & Charru, F. (2010). Bed load transport in turbulent flow at the grain scale: Experiments and modeling. *Journal of Geophysical Research*, *115*, F04001. https://doi.org/10.1029/2009JF001628

Lee, H. Y., Chen, Y. H., You, J. Y., & Lin, Y. T. (2000). Investigations of continuous bed load saltating process. *Journal of Hydraulic Engineering*, *126*(9), 691–700. https://doi.org/10.1061/(ASCE)0733-9429(2000)126:9(691)

Lisle, I. G., Rose, C. W., Hogarth, W. L., Hairsine, P. B., Sander, G. C., & Parlange, J. Y. (1998). Stochastic sediment transport in soil erosion. *Journal of Hydrology*, *204*(1-4), 217–230. https://doi.org/10.1016/S0022-1694(97)00123-6

Martin, R. L., Jerolmack, D. J., & Schumer, R. (2012). The physical basis for anomalous diffusion in bed load transport. *Journal of Geophysical Research*, *117*, F01018. https://doi.org/10.1029/2011JF002075

Nelson, J. M., Shreve, R. L., McLean, S. R., & Drake, T. G. (1995). Role of near-bed turbulence in bed load transport and bed form mechanics. *Water Resources Research*, *31*(8), 2071–2086. https://doi.org/10.1029/95WR00976

Nikora, V., Habersack, H., Huber, T., & McEwan, I. (2002). On bed particle diffusion in gravel bed flows under weak bed load transport. *Water Resources Research*, *38*(6), 1081. https://doi.org/10.1029/2001WR000513

Nikora, V., Heald, J., Goring, D., & McEwan, I. (2001). Diffusion of saltating particles in unidirectional water flow over a rough granular bed. *Journal of Physics A: Mathematical and General*, *34*(50), L743–L749. https://doi.org/10.1088/0305-4470/34/50/103

Niño, Y., & Garcia, M. (1998). Using Lagrangian particle saltation observations for bedload sediment transport modelling. *Hydrological Processes*, *12*(8), 1197–1218. https://doi.org/10.1002/(SICI)1099-1085(19980630)12:8%3C1197::AID-HYP612%3E3.0.CO;2-U

Papanicolaou, A. N., Diplas, P., Evaggelopoulos, N., & Fotopoulos, S. (2002). Stochastic incipient motion criterion for spheres under various bed packing conditions. *Journal of Hydraulic Engineering*, *128*(4), 369–380. https://doi.org/10.1061/(ASCE)0733-9429(2002)128:4(369)

Radice, A. (2009). Use of the Lorenz curve to quantify statistical nonuniformity of sediment transport rate. *Journal of Hydraulic Engineering*, *135*(4), 320–326. https://doi.org/10.1061/(ASCE)0733-9429(2009)135:4(320)

Radice, A., & Ballio, F. (2008). Double-average characteristics of sediment motion in one-dimensional bed load. *Acta Geophysica*, *56*(3), 654–668. https://doi.org/10.2478/s11600-008-0015-0

Radice, A., Ballio, F., & Nikora, V. (2009). On statistical properties of bed-load sediment concentration. *Water Resources Research*, *45*, W06501. https://doi.org/10.1029/2008WR007192

Radice, A., Ballio, F., & Nikora, V. (2010). Statistics and characteristic scales for bed load in a channel flow with sidewall effects. *Acta Geophysica*, *58*(6), 1072–1093. https://doi.org/10.2478/s11600-010-0020-y

Radice, A., Nikora, V., Campagnol, J., & Ballio, F. (2013). Active interactions between turbulence and bed load: Conceptual picture and experimental evidence. *Water Resources Research*, *49*, 90–99. https://doi.org/10.1029/2012WR012255

Radice, A., Sarkar, S., & Ballio, F. (2017). Image-based Lagrangian particle tracking in bed-load experiments. *Journal of Visualized Experiments*, *125*(125), e55874. https://doi.org/10.3791/55874

Ramesh, B., Kothyari, U. C., & Murugesan, K. (2011). Near-bed particle motion over transitionally-rough bed. *Journal of Hydraulic Research*, *49*(6), 757–765. https://doi.org/10.1080/00221686.2011.620369

Roseberry, J. C., Schmeeckle, M. W., & Furbish, D. J. (2012). A probabilistic description of the bed load sediment flux: 2. Particle activity and motions. *Journal of Geophysical Research*, *117*, F03032. https://doi.org/10.1029/2012JF002353

Seizilles, G., Lajeunesse, E., Devauchelle, O., & Bak, M. (2014). Cross-stream diffusion in bedload transport. *Physics of Fluids*, *26*(1), 013302. https://doi.org/10.1063/1.4861001

Singh, A., Fienberg, K., Jerolmack, D. J., Marr, J., & Foufoula-Georgiou, E. (2009). Experimental evidence for statistical scaling and intermittency in sediment transport rates. *Journal of Geophysical Research*, *114*, F01025. https://doi.org/10.1029/2007JF000963

Turowski, J. M. (2010). Probability distributions of bed load transport rates: A new derivation and comparison with field data. *Water Resources Research*, *46*, W08501. https://doi.org/10.1029/2009WR008488

Van Rijn, L. C. (1984). Sediment pick-up functions. *Journal of Hydraulic Engineering*, *110*(10), 1494–1502. https://doi.org/10.1061/(ASCE)0733-9429(1984)110:10(1494)

Voepel, H., Schumer, R., & Hassan, M. A. (2013). Sediment residence time distributions: Theory and application from bed elevation measurements. *Journal of Geophysical Research: Earth Surface*, *118*, 2557–2567. https://doi.org/10.1002/jgrf.20151

Von Plato, J. (1991). Boltzmann's ergodic hypothesis. *Archive for History of Exact Sciences*, *42*(1), 71–89. https://doi.org/10.1007/BF00384333

Wu, F. C., & Chou, Y. J. (2003). Rolling and lifting probabilities for sediment entrainment. *Journal of Hydraulic Engineering*, *129*(2), 110–119. https://doi.org/10.1061/(ASCE)0733-9429(2003)129:2(110)